NONLINEAR GREY-BOX IDENTIFICATION OF INDUSTRIAL ROBOTS CONTAINING FLEXIBILITIES [1]

Erik Wernholt and Svante Gunnarsson

Dept. of Electrical Engineering, Linköping University,
SE-581 83 Linköping, Sweden

Abstract: Nonlinear grey-box identification of industrial robots is considered. A three-step identification procedure is proposed in which parameters for rigid body dynamics, friction, and flexibilities can be identified only using measurements on the motor. In the first two steps, good initial parameter estimates are derived which are used in the last step, where the parameters of a nonlinear physically parameterized model are identified directly in the time domain. The procedure is exemplified using real data from an experimental industrial robot.

Keywords: Identification, Robotics, Flexible arms, Friction, Manipulators

1. INTRODUCTION

System identification in robotics is a vast research area and can be divided into, at least, three different levels or application areas. These levels involve the estimation of the kinematic description, the dynamic model (often divided into rigid body and flexible body dynamics), and the joint model (*e.g.*, motor inertia, gearbox elasticity and backlash, motor characteristics, and friction parameters). Some results on the latter two areas are mentioned in Section 4. An overview of identification in robotics can also be found in (Kozlowski, 1998).

Nominal parameter values can, for the kinematics and rigid body dynamics, often be obtained from CAD models. Most of the joint model parameters are often measured in a test bench. Flexibilities and friction parameters are harder to find and therefore tuned after assembly. However, to obtain high accuracy, all parameters must usually be tuned by the use of experimental data. The development rate of new industrial robots is also high, with several kinds of robots and different configurations to tune each year. For top performance, there could also be a need to re-tune robots at the customer site due to wear or other changing conditions. This means that there is an increasing need for good identification procedures.

In the work presented here, a three-step identification procedure is proposed in which parameters for rigid body dynamics, friction, and flexibilities can be identified only using measurements on the motor side of the flexibility. The main point is the last step, where the parameters of a nonlinear physically parameterized model (a nonlinear grey-box model) are identified directly in the time domain. The first two steps give special attention to the problem of finding good initial parameter estimates for the iterative optimization routine. The procedure is exemplified using real data from an experimental industrial robot.

The work reported here is closely related to the problems considered in, for example, (Östring *et al.*, 2003; Isaksson *et al.*, 2003). In (Östring *et al.*, 2003), a method is applied where inertial parameters as well as parameters describing the flexibility can be identified directly in the time domain. This is done by utilizing a user-defined model structure in the System Identification Toolbox (SITB). However, only linear models were considered in their work. (Isaksson *et al.*, 2003)

[1] Supported by VINNOVA's Center of Excellence ISIS at Linköping University.

consider grey-box identification of a two-mass model with backlash, where black-box modeling is used to find initial parameter values.

The paper is organized as follows. In Section 2 the nonlinear grey-box identification problem is briefly described and Section 3 shows the nonlinear robot model used for identification. The three-step identification procedure is presented in Section 4. In Section 5 the data collection is described, and Section 6 shows the results from applying the proposed identification procedure to the experimental data. Finally, Section 7 contains some conclusions and notes on future work.

2. NONLINEAR GREY-BOX IDENTIFICATION

The starting point for the nonlinear grey-box identification is the continuous time state space model structure

$$\dot{x}(t) = f(t, x(t), \theta, u(t)) \tag{1a}$$
$$y(t) = h(t, x(t), \theta, u(t)) + e(t) \tag{1b}$$

where f and h are nonlinear functions. $x(t)$ is the state vector, $u(t)$ and $y(t)$ are input and output signals, $e(t)$ a white measurement disturbance signal, and t denotes time. Finally θ is the vector of unknown parameters. Given a set of input/output-data the aim is to determine the parameter vector that minimizes a criterion like

$$V_N(\theta) = \frac{1}{N}\sum_{t=1}^{N} \varepsilon^2(t, \theta) \tag{2}$$

where $\varepsilon(t)$ denotes the prediction error

$$\varepsilon(t, \theta) = y(t) - \hat{y}(t, \theta) \tag{3}$$

The experiments presented in this paper will utilize the nonlinear grey-box model structure NLGREY, available in a beta version of a nonlinear extension to the System Identification Toolbox (SITB), (Ljung, 2003). The model structure NLGREY is similar to the IDGREY model structure in SITB. The model can be either a discrete or continuous time state space model, and it is defined in a Matlab m-file/mex-file. In the current version of the software, only OE-models can be used, *i.e.* only additive white noise, $e(t)$, on the output. The prediction $\hat{y}(t|\theta)$ then becomes the simulated output of the model (1) with the input $u(t)$ (without $e(t)$) for the current parameter vector θ. The data set, $\{y, u\}$, is put into an IDDATA object and θ is estimated by applying a prediction error method, which performs a numerical optimization of the criterion (2) by an iterative numerical search algorithm. This search algorithm involves simulation of the system for different values of θ. The user specifies an initial parameter vector and it is also possible to fix some components in θ. To speed up the numerical optimization, the simulation model is implemented in a mex-file (C-code).

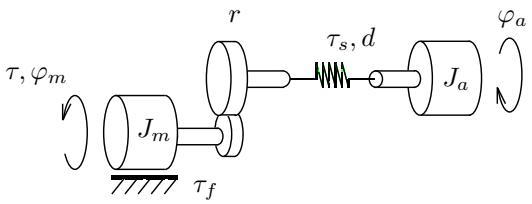

Fig. 1. The two-mass flexible model of the robot arm.

3. ROBOT MODEL

The industrial robot that will be studied in this paper is, for movements around an axis not affected by gravity, modeled by a nonlinear two-mass flexible model which is illustrated in Figure 1. A two-mass model is probably too simple to describe the true system (see, for example, (Östring *et al.*, 2003) or Figure 3), but it can still be used as an illustration of the proposed identification procedure.

The differential equations describing the dynamics of the robot arm are

$$J_m\ddot{\varphi}_m + rd(r\dot{\varphi}_m - \dot{\varphi}_a) + \tau_f + r\tau_s = \tau \tag{4}$$
$$J_a\ddot{\varphi}_a - d(r\dot{\varphi}_m - \dot{\varphi}_a) - \tau_s = 0 \tag{5}$$

where J_m and J_a are the moments of inertia of the motor and arm respectively, r is the gear ratio, τ is the motor torque and d is the damping parameter. The spring and gear friction torques, τ_s and τ_f respectively, are often approximately modeled by linear models (see, for example, (Östring *et al.*, 2003)). In this work, nonlinear models will be used to capture the effect of the Coulomb friction and to get a more realistic model of the spring. The torque of the spring is modeled as

$$\tau_s = k_1(r\varphi_m - \varphi_a) + k_3(r\varphi_m - \varphi_a)^3 \tag{6}$$

where φ_m and φ_a are the angles of the motor and arm respectively, and k_1 and k_3 are the parameters of the spring. The torque due to friction is modeled as

$$\tau_f = F_v\dot{\varphi}_m + F_c\,\mathrm{sgn}(\dot{\varphi}_m) \tag{7}$$

where F_v and F_c are the viscous and Coulomb friction coefficients. A third nonlinearity of practical importance is the presence of backlash in the gearbox, but this problem is left for future work. See also (Isaksson *et al.*, 2003). Using (4) to (7), a nonlinear state space model of the system can be derived. The motor torque, τ, is used as input, u, and with the states defined as

$$x = \begin{pmatrix} x_1 \\ x_2 \\ x_3 \end{pmatrix} = \begin{pmatrix} r\varphi_m - \varphi_a \\ \dot{\varphi}_m \\ \dot{\varphi}_a \end{pmatrix} \tag{8}$$

the state space equations become

$$\dot{x}_1 = rx_2 - x_3 \tag{9a}$$
$$\dot{x}_2 = \frac{1}{J_m}\Big(- F_v x_2 - F_c\,\mathrm{sgn}(x_2) - rd(rx_2 - x_3) - rk_1x_1 - rk_3x_1^3 + u\Big) \tag{9b}$$
$$\dot{x}_3 = \frac{1}{J_a}\Big(d(rx_2 - x_3) + k_1x_1 + k_3x_1^3\Big) \tag{9c}$$

4. IDENTIFICATION PROCEDURE

The aim is to identify all parameters in the robot model, described in Section 3, using experimental data and the nonlinear grey-box identification procedure described in Section 2. An inherent problem of iterative search routines is that only convergence to a local minimum can be guaranteed. In order to converge to the global minimum, a good initial parameter estimate is important. Therefore a three-step identification procedure is proposed where the first two steps find initial parameter values and in the third step, the nonlinear grey-box identification procedure is applied.

4.1 Step 1: Initial values for rigid body dynamics and friction

There exists a vast amount of literature on the identification of the rigid body dynamics, see, for example, (Grotjahn *et al.*, 2001; Gautier and Poignet, 2001; Swevers *et al.*, 1997; Pfeiffer and Hölzl, 1995). The standard procedure includes a dynamic model, linear in the parameters, that is characterized by ten inertial parameters per link. This representation is redundant, but there are methods to find a minimal dimensional parameter vector, called *base parameters*, that characterize the dynamic model. Usually a friction model with two parameters per link is used, describing viscous and Coulomb friction. This model is not sufficient to correctly describe dynamic friction, see (Armstrong-Hélouvry *et al.*, 1994), but compensates the major frictional effects on the identification of rigid body dynamics. The robot is moved along some (optimized) trajectory and applied torque and joint movements are recorded. The parameters are then estimated using linear regression. Since the main interest here is to find initial values, parts of this step could also be replaced by nominal values from CAD models. If, on the other hand, (some) parameters can be estimated with high accuracy in this step, they could be fixed during the third step, leading to a lower dimensional iterative search.

For the robot model in Section 3, the rigid body dynamics and friction is

$$(J_m + r^2 J_a)\ddot{\varphi}_m + F_v\dot{\varphi}_m + F_c \operatorname{sgn}\dot{\varphi}_m = \tau \quad (10)$$

which can be written as linear regression

$$\begin{pmatrix}\ddot{\varphi}_m & \dot{\varphi}_m & \operatorname{sgn}\dot{\varphi}_m\end{pmatrix}\begin{pmatrix}J_m + r^2 J_a \\ F_v \\ F_c\end{pmatrix} = \tau \quad (11)$$

The parameter vector can then be determined as the solution to a standard least-squares problem.

4.2 Step 2: Initial values for flexibilities

The major flexibility in an industrial robot is normally located at the joint level, due to the transmission. A two-mass model (or coupled two-mass models for multivariable cases) is then sufficient to describe the dynamics. Weaker (more compliant) robot structures will in addition introduce significant flexibilities in the links and their connections. Therefore higher order models are sometimes needed in order to get a sufficient description of the system. Many different methods are described in the literature (Behi and Tesar, 1991; Ferretti *et al.*, 1994; Pfeiffer and Hölzl, 1995; Johansson *et al.*, 2000; Albu-Schäffer and Hirzinger, 2001). They differ in, for example, assumed model structure, required measurement signals, and complexity of the identification method.

Identification of flexibilities is more involved than the identification of rigid body dynamics. The main reason is that now typically only a subset of the state variables are measured and one can therefore not use linear regression. This could of course be solved by adding sensors, see, *e.g.*, (Pfeiffer and Hölzl, 1995), where joint parameters are estimated by fixation of the links in fixtures and using force sensors, or (Albu-Schäffer and Hirzinger, 2001), where joint torque sensors are used. These solutions are expensive and the experiments quite involved and therefore not desirable if a simpler solution exists. In (Berglund and Hovland, 2000), an interesting method is described for the identification of masses, springs and dampers, only using applied torque and joint movements. The identification is based on an estimated Frequency Response Function (FRF) in combination with the solution of an inverse eigenvalue problem. See also (Hovland *et al.*, 2001) for an extension to systems containing coupled inertia terms, which is the case for multivariable systems. Here, a simplified method will be used to obtain initial values for the flexibilities in the two-mass model, see Section 6.2. One could also apply the method proposed in (Isaksson *et al.*, 2003), based on black-box identification.

4.3 Step 3: Nonlinear grey-box identification

Combining the estimates from step 1 and 2 gives an initial parameter estimate, and the nonlinear grey-box identification method described in Section 2 can now be applied.

5. DATA COLLECTION

The data used for identification are real data collected from an experimental robot. For this kind of application it is necessary to use feedback control while data are collected, both for safety reasons and in order to keep the robot around its operation point. An experimental control system is used, which makes it possible to use off-line computed reference signals for the joint controllers. The identification will therefore be carried out using closed loop data, which might lead to biased estimates (see (Ljung, 1999) for details).

For the different steps in the identification procedure, different excitation signals are needed. In step 1, the rigid body dynamics and friction parameters should be excited without introducing any oscillations due to the flexibilities. Therefore a low frequency excitation is preferred. In step 2, on the other hand, the whole frequency band should be excited where notch and peak frequencies in the frequency response function are expected. The influence of static friction should also be reduced, so a broadband excitation with as few zero velocity crossings as possible is selected. Finally, for step 3 a data set (or a combination of data sets) is needed that excite all free parameters in the model.

The properties of the excitation signal will of course affect the quality of the estimated parameters. Since the system is nonlinear, not only the spectrum will matter, but also the amplitude and the actual waveforms. It is common to optimize the excitation signal according to some criterion, see, for example, (Swevers *et al.*, 1997), but that is outside the scope of this paper. The following three excitation signals will be used as reference speed, φ_m^{ref}, for the controller. They are all sampled at 2 kHz ($T = 0.5$ ms).

Data set 1: Triangle wave signal, 6.25 s of data, with amplitude 40 rad/s and period time 5 s.

Data set 2: Multisine signal (sum of sinusoids), 5 s of data, with flat amplitude spectrum in the frequency interval 1-40 Hz with a crest factor of 1.55, period time 5 s and a peak value of 5 rad/s. The multisine signal is superimposed on a square wave with amplitude 8 rad/s and period time 5 s.

Data set 3: Similar to data set 2, but the multisine signal has a peak value of 10 rad/s and the amplitude of the square wave is 12 rad/s.

The last two data sets mainly differ in amplitude and can therefore be used to see nonlinear effects on the estimates. For details on the excitation signals, see, *e.g.* (Pintelon and Schoukens, 2001; Ljung, 1999).

6. RESULTS

The physical parameters in the robot model from Section 3 will here be identified by applying the proposed three-step identification procedure from Section 4, using the experimental data described in Section 5. The gear ratio $r = 1/224.3$ is known.

6.1 Step 1

Using data set 1 together with the linear regression (11) gives the following parameter estimates

$$\begin{pmatrix} J_m + r^2 J_a \\ F_v \\ F_c \end{pmatrix} = \begin{pmatrix} 0.0280 \\ 0.0136 \\ 0.642 \end{pmatrix} \tag{12}$$

The velocity and acceleration used in the regressor, see (11), are obtained from position measurements using non-causal low-pass filtering (filtfilt in Matlab) and central difference algorithms.

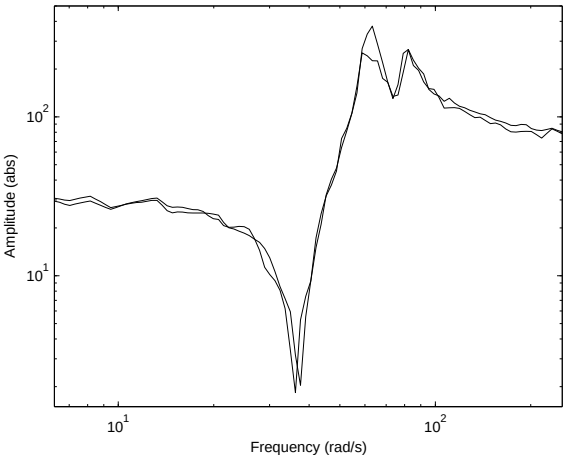

Fig. 2. Magnitude of the FRF for data sets 2 (thin line) and 3 (thick line) from motor torque to motor acceleration.

6.2 Step 2

The FRFs for data sets 2 and 3 from motor torque to motor acceleration can be seen in Figure 2. Note especially that the notch frequency is higher for the data set with larger amplitude. For a linear system, these estimates should be similar (except for noise). For a linear two-mass model, the approximate transfer function (ignoring the damping, d) from motor torque to motor acceleration is given by

$$\frac{s(J_a s^2 + k)}{s^3 J_a J_m + s^2 J_a F_v + s \cdot k(J_m + r^2 J_a) + k F_v} \tag{13}$$

with $1/J_m$ as the high frequency gain and $\omega_n = \sqrt{k/J_a}$ as the notch frequency. Using the FRFs in Figure 2, the following numerical values are achieved. For data set 2, $J_m^{[2]} = 0.0126$ and $\omega_n^{[2]} = 35.19$, and for data set 3, $J_m^{[3]} = 0.0120$ and $\omega_n^{[3]} = 37.70$. The estimate of J_m is taken as the average value for the two data sets, $J_m = 0.0123$. Since the gear ratio, r, is known, an estimate $J_a = 790$ is found by combining (12) and $J_m = 0.0123$. Knowing J_a, the spring stiffness $k^{[i]}$ for data set i is derived by using the approximate relation $\omega_n^{[i]} = \sqrt{k^{[i]}/J_a}$, which for the two data sets gives $k^{[2]} = 9.78 \cdot 10^5$ and $k^{[3]} = 1.12 \cdot 10^6$. Since the two amplitudes give different spring constants, it is probably fair to conclude that there is a nonlinear effect present in the experimental data. The damping is hard to estimate and its initial value is here simply set to zero.

For a higher order model and/or a multivariable model, the procedure described in (Hovland *et al.*, 2001) can be used in this step.

To find initial estimates for k_1 and k_3, the following ad hoc procedure is used. The spring constant k from the FRFs can, in some sense, be regarded as an "average

Table 1. Estimated parameters, where the initial model `m0` comes from the first two steps and the other models are estimated in the third step using the denoted data sets. For the `m3` model, the standard deviation of the parameter estimate is included as well.

Model:	`m0`	`m1`	`m2`	`m3`
Est. data:	Init.	1,2	1,3	1,2,3
J_m $(\times 10^2)$	1.23	1.26	1.22	1.21 ± 0.00181
J_a $(\times 10^{-3})$	0.79	1.07	1.11	1.13 ± 0.00209
k_1 $(\times 10^{-6})$	0.814	1.42	1.46	1.46 ± 0.00346
k_3 $(\times 10^{-10})$	5.4	3.77	4.69	3.72 ± 0.186
d $(\times 10^{-3})$	0	2.73	3.08	2.63 ± 0.0488
F_v $(\times 10^2)$	1.36	1.18	1.36	1.30 ± 0.00235
F_c $(\times 10^1)$	6.42	6.68	6.23	6.44 ± 0.00488

Table 2. Model fit when validating estimated models on data sets 1,2 and 3.

	`m0`	`m1`	`m2`	`m3`
Data set 1	84.44	97.12	97.46	96.39
Data set 2	32.8	61.54	60.59	62.33
Data set 3	49.95	74.43	74.42	74.94

spring constant". Reasonable estimates for k_1 and k_3 can then be found by minimizing

$$\sum_{i=2}^{3}\sum_{t=1}^{N}\left(\left(k^{[i]}x_1^{[i]}(t) - k_1 x_1^{[i]}(t) - k_3(x_1^{[i]}(t))^3\right)^2\right) \tag{14}$$

where $k^{[i]}$ and $x_1^{[i]}(t)$ are the estimated spring constants and spring deflection, respectively, for data sets $i = 2, 3$. Since the state x_1 is not measured, it is simulated using the model (9) with the estimated nominal parameters and a linear spring model $\tau_s = kx_1$.

6.3 Step 3

Combining the estimates from steps 1 and 2 gives the initial model `m0` in Table 1. The quality of the estimated models is assessed using the model fit

$$\text{fit} = 100\left(1 - \frac{\sqrt{\sum_{t=1}^{N}(y(t) - \hat{y}(t))^2}}{\sqrt{\sum_{t=1}^{N}(y(t) - \bar{y})^2}}\right) \tag{15}$$

where $y(t)$ is the measured output (the motor velocity), $\hat{y}(t)$ is the simulated output and $\bar{y}$ is the mean value of the measured output. For the estimation, data set 1 is combined with data sets 2 and/or 3 (using merge in SITB) according to Table 1. Including data set 1 is motivated by the fact that if only data sets 2 and/or 3 are used, the model fit is improved when validating on data sets 2 and 3, but the estimated parameters are unrealistic (*e.g.*, negative Coulomb friction) and the model fit for data set 1 is low. The optimization is carried out for 30 iterations, giving parameter estimates and models shown in Table 1. The estimated models are validated using the three data sets and the model fit is given in Table 2.

Comparing the model fit for the different models in Table 2, one can notice that the model fit is substantially improved by the nonlinear grey-box identification step. However, to be fair, the initial estimates from step 1 and 2 (the `m0` model) could probably be improved by using optimal excitation. There are no major differences in model fit when validating with estimation data compared to cross validation. This is also reasonable since the signal-to-noise ratio is quite large. For the `m3` model, the relative importance of data set 1 gets lower, which also shows up in the increased model fit for data sets 2 and 3.

Table 3. Difference in model fit for the `m3` model, compared to Table 2, when each parameter is perturbed $+20\%/-20\%$.

	Data set 1	Data set 2	Data set 3
J_m	$-4.51/-0.81$	$0.77/-8.09$	$-0.94/-10.7$
J_a	$-8.51/-5.34$	$5.03/-9.45$	$1.08/-7.36$
k_1	$0.13/\ 0.02$	$-2.73/-2.55$	$-3.93/-4.14$
k_3	$-0.01/-0.01$	$-0.05/\ 0.06$	$-0.11/\ 0.08$
d	$0.03/-0.06$	$-0.09/\ 0.02$	$0.12/-0.38$
F_v	$-5.79/-1.65$	$2.46/-4.23$	$0.70/-1.84$
F_c	$-14.7/-8.23$	$-0.11/-21.5$	$-1.25/-9.13$

To analyze the relative importance on the model fit for each parameter, the estimated model `m3` is used and each parameter is perturbed $\pm 20\%$, one at a time. In Table 3 the difference in model fit can be seen for the three data sets. For data set 1, one can note that the parameters describing the flexibility have a small influence, compared to the rigid body dynamics and friction parameters. The nonlinear stiffness parameter, k_3, does not significantly affect the model fit. Removing it gives almost no reduction in model fit. This is a puzzling result, since estimated FRFs (see Figure 2) as well as test bench measurements show an amplitude dependent gearbox stiffness. A more detailed analysis of how the nonlinearities affect the estimate is therefore needed, including more experiments and other model structures.

As an alternative sensitivity analysis, the covariance matrix for the estimated parameters can also be studied. The asymptotic accuracy of a certain parameter relates to how the parameter affects the predicted model output. Loosely speaking, $\mathrm{E}\, V_N'(\theta)[V_N'(\theta)]^T$ will asymptotically be proportional to the inverse of the parameter covariance matrix (see (Ljung, 1999) for a thorough treatment). Comparing the standard deviations in Table 1 also shows that the k_3 parameter, and to some extent the damping d, are hard to accurately estimate.

In Figure 3 a Bode diagram for the estimated model `m3`, ignoring the nonlinear model parameters (k_3 and F_c), can be seen together with the estimated FRFs for data sets 2 and 3. One can clearly see the close correspondence, which further validates the estimated model. However, to capture the two resonance peaks around 60 and 80 rad/s in the FRF, (at least) a three-mass model would be needed.

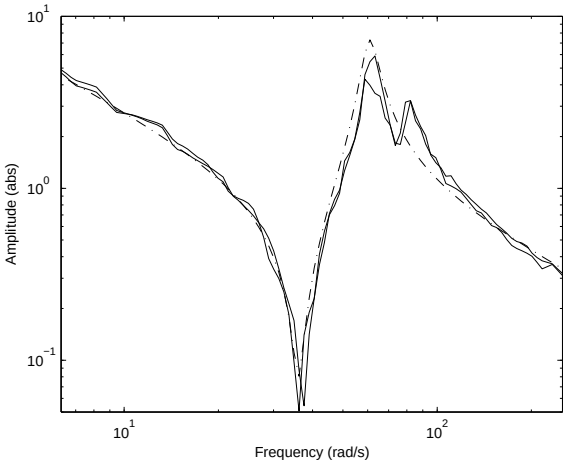

Fig. 3. Magnitude of the FRF for data sets 2 (thin line) and 3 (thick line) from motor torque to motor velocity together with the estimated model `m3` (dash-dotted line).

7. CONCLUSIONS

A three-step identification procedure has been proposed for the identification of rigid body dynamics, friction, and flexibilities, only using measurements on the motor side. The procedure has been exemplified using experimental data from an industrial robot together with a flexible two-mass model where nonlinear spring stiffness and Coulomb friction have been added. The estimated physical parameters have realistic numerical values and give a model with high model fit and fairly good correspondence to FRF measurements. However, the nonlinear spring stiffness is not significant in the selected data sets.

There are a number of aspects of the presented results that are subjects for future work. One important problem is to find a model structure that explains the amplitude dependent properties of the system. This will probably involve higher order models as well as additional nonlinearities. A further topic is to apply the method to a multivariable system. There are no principal problems in the proposed identification procedure, but the last step involving the iterative numerical search would be more time consuming and perhaps numerically sensitive since the system is highly resonant.

REFERENCES

Albu-Schäffer, A. and G. Hirzinger (2001). Parameter identification and passivity based joint control for a 7DOF torque controlled light weight robot. In: *Proceedings of the 2001 IEEE International Conference on Robotics and Automation*. Seoul, Korea. pp. 2852–2858.

Armstrong-Hélouvry, B., P. Dupont and C. Canudas de Wit (1994). A survey of models, analysis tools and compensation methods for the control of machines with friction. *Automatica* **30**(7), 1083–1138.

Behi, F. and D. Tesar (1991). Parametric identification for industrial manipulators using experimental modal analysis. *IEEE Trans. Robot. Automat.* **7**(5), 642–652.

Berglund, E. and G. E. Hovland (2000). Automatic elasticity tuning of industrial robot manipulators. In: *Proceedings of the 39th IEEE Conference on Decision and Control*. Sydney, Australia. pp. 5091–5096.

Ferretti, G., G. Magnani and P. Rocco (1994). Estimation of resonant transfer functions in the joints of an industrial robot. In: *2nd IFAC Symposium on Intelligent Control and Control Applications, SICICA 94*. Vol. 1. Budapest. pp. 371–376.

Gautier, M. and P. Poignet (2001). Extended kalman filtering and weighted least squares dynamic identification of robot. *Control Engineering Practice* **9**(12), 1361–1372.

Grotjahn, M., M. Daemi and B. Heimann (2001). Friction and rigid body identification of robot dynamics. *International Journal of Solids and Structures* **38**, 1889–1902.

Hovland, G. E., E. Berglund and S. Hanssen (2001). Identification of coupled elastic dynamics using inverse eigenvalue theory. In: *Proceedings of the 32nd ISR (International Symposium on Robotics)*. pp. 1392–1397.

Isaksson, A., R. Lindkvist, X. Zhang, M. Nordin and M. Tallfors (2003). Identification of mechanical parameters in drive train systems. In: *IFAC System Identification Symposium SYSID 2003*.

Johansson, R., A. Robertsson, K. Nilsson and M. Verhaegen (2000). State-space system identification of robot manipulator dynamics. *Mechatronics* **10**(3), 403–418.

Kozlowski, K. (1998). *Modelling and Identification in Robotics*. Springer-Verlag.

Ljung, L. (1999). *System Identification: Theory for the User*. 2nd ed. Prentice Hall. Upper Saddle River, New Jersey, USA.

Ljung, L. (2003). *System Identification Toolbox – User's Guide*. The MathWorks Inc. Sherborn, MA, USA.

Pfeiffer, F. and J. Hölzl (1995). Parameter identification for industrial robots. In: *Proceedings of the 1995 IEEE International Conference on Robotics and Automation*. Vol. 2. Nagoya, Japan. pp. 1468–1476.

Pintelon, R. and J. Schoukens (2001). *System identification: a frequency domain approach*. IEEE Press. New York.

Swevers, J., C. Ganseman, D. B. Tükel, J. De Schutter and H. Van Brussel (1997). Optimal robot excitation and identification. *IEEE Trans. Robot. Automat.* **13**(5), 730–740.

Östring, M., S. Gunnarsson and M. Norrlöf (2003). Closed-loop identification of an industrial robot containing flexibilities. *Control Engineering Practice* **11**, 291–300.